

Development of wrought precipitation strengthened IN939 superalloy

M. R. Jahangiri^{*1,2}, H. Arabi^{1,3} and S. M. A. Boutorabi^{1,3}

The potential of cast IN939 superalloy to be converted to wrought alloy has been explored in the present work. For this objective, bars of cast alloy were rolled under different conditions and then subjected to various heat treatment cycles. The results indicated that the yield strength, ultimate tensile strength and ductility of the wrought IN939 alloy are superior to the cast version. The stress rupture properties of wrought IN939 superalloy are better than those of the widely used superalloys, such as Nimonic 90 and Waspaloy, and approach the alloy Nimonic 105 properties. This is very notable because Nimonic 105 contains ~45 vol.-% γ' that is much greater than the volume fraction of those strengthening precipitates in the alloy IN939 (~35%). On the whole, the wrought form of this alloy has a high potential for manufacturing hot components to be used safely under aggressive turbine environment.

Keywords: Nickel base superalloys, IN939, Cast, Wrought, Microstructure, Mechanical properties

Introduction

Wrought and cast nickel base superalloys are frequently used in hot sections of gas turbines. This is due to their high strength and corrosion resistance at high temperatures as well as their relatively low manufacturing cost.^{1,2}

Wrought precipitation strengthened Ni–Cr–Co superalloys combine exceptional oxidation resistance with mechanical properties at high temperatures.^{1–3} One of the most important precipitation strengthened Ni–Cr–Co superalloys that has been widely used in manufacturing gas turbine hot section parts is Waspaloy. Owing to the need for alloys with higher creep or corrosion resistance, superalloys such as Rene 41, Udimet 520, Udimet 720 and Rene 88 have been later developed by changing the amounts of some alloying elements such as Ti, Al and Mo in Waspaloy composition. All these new alloys are often used in wrought condition.³ The powder metallurgy and cast/wrought routes are the main processes for manufacturing turbine components from Ni–Cr–Co based superalloys. These alloys can be used in applications such as turbine blades and vanes, discs, rotors, casings, fasteners, etc.

IN939 is a relatively new precipitation hardened Ni–Cr–Co superalloy which has been developed by modification of Waspaloy. At present, this alloy is used as a cast alloy in manufacturing gas turbine blades/vanes and other structural parts such as burner nozzles and turbine casings.⁴ It is one of the best alloys among the hot

corrosion and oxidation resistant alloys having desirable mechanical properties. Although considerable investigations have been carried out on the microstructure and mechanical properties of this alloy in the as cast and heat treated condition,^{4–7} there are no published data dealing with the microstructure and mechanical properties of this alloy in wrought form. Therefore, IN939 might not have been used in wrought form so far.

In addition to the high amount of Cr, IN939 has a large amount of Co. This can prevent η phase formation during hot working or subsequent heat treatment cycles.⁸ The Ti/Al weight ratio for IN939 is ~2, and this enhances the corrosion resistance of the alloy.⁹ Owing to the high content of Ti in the alloy, the role of this alloying element to form γ' precipitates is essential, and this provides higher strength at higher temperatures for the alloy.^{10–12}

Based on the published data reported for the cast IN939 superalloy,^{4,6,7} it could be predicted that the wrought version of this alloy would have excellent hot corrosion and oxidation resistance, low tendency to form topologically closed packed phases such as σ and μ due to low Nv factor and absence of Mo in its chemical composition.^{12,13}

The IN939 superalloy has high amounts of carbide forming elements, such as Ti, Nb and Ta, but there is no Mo in its chemical composition. MC carbides, which are free from Mo, can enhance the fatigue life of the alloy.¹⁴ γ and γ' phases in the microstructure of the alloy provide high strength due to the presence of appropriate amounts of elements W, Ta and Nb,¹⁵ and the process of making wrought alloy provides appropriate yield strength and creep properties due to the presence of the elements W and Ta and the absence of Mo in the alloy composition.¹⁶ Finally, one can predict the superior weldability of this wrought alloy compared to alloys containing higher contents of Al and Ti and lower

¹School of Metallurgy and Materials Engineering, Iran University of Science and Technology (IUST), Tehran 16846-13114, Iran

²Metallurgy Department, Niroo Research Institute, Tehran 14686, Iran

³Center of Excellence for Advanced Materials & Processing, IUST, Tehran, Iran

*Corresponding author, email jahangiri@iust.ac.ir

content of Co according to published data.¹⁷ In effect, reducing the Al and Ti contents of the alloy leads to the reduction of inter- and intragranular liquation of second phases such as γ' precipitates, MC carbides and eta phase, and this can enhance the weldability¹⁸ as well as hot workability of the alloy.

Among the well known wrought Ni–Cr–Co superalloys that have been developed to be used at temperatures up to 900–950°C are Nimonic 90 and 105.^{19,20} These alloys are currently used in the manufacturing of gas turbine parts such as blades, discs and other forged components. Nimonic 105 alloy contains 4.5–5 wt.%Al and 5 wt.%Mo and shows less corrosion resistance and weldability compared to IN939 alloy. Inconel alloy 740 is a recently developed Ni–Cr–Co precipitation strengthened superalloy with a potential to be used at temperatures up to 800°C. By virtue of its high Cr content, the alloy demonstrates excellent corrosion resistance compared to the best existing Ni base superalloys.^{21,22}

The aim of the present paper is to develop wrought IN939 superalloy and to compare its tensile strength and creep rupture properties with other widely used wrought superalloys such as Waspaloy, Nimonic 90 and Nimonic 105.

Experimental

To prepare the wrought IN939 alloy, the virgin IN939 master alloy was melted in a vacuum induction furnace under a vacuum of 10^{-3} mbar, and ingots with the composition of Ni–0.144C–19.25Co–22.38Cr–3.65Ti–1.99Al–1.97W–1.45Ta–0.99Nb–0.09Zr–0.011B–0.002P–0.001S (wt-%) were cast. The pouring temperature was 1460°C. The ingot dimensions were 80 × 60 × 24 mm. After two-stage homogenisation annealing (first 20 h at 1125°C followed by 10 h at 1200°C) for complete dissolution of η phase, preventing incipient melting and improving hot workability,^{23,24} the ingots were hot rolled. Temperatures and thickness reductions in the hot rolling procedures were selected based on the results of hot compression experiments of the alloy (which are not given in the present paper). At first, the ingots were hot rolled in total of 40% at 1150°C with five passes, each of which has ~10% reduction in thickness, with a 10 min reheat between each pass to maintain the temperature at 1150°C. Then, the specimens were hot rolled for 35 and 30% at 1100 and 1050°C respectively with the same rolling schedule and appropriate pass numbers. The last pass was followed by air cooling. There was not any evidence of cracking on the edges or corners of the rolled strips. The final thickness of the hot rolled strips was 6.5 mm.

The hot rolled strips were then heat treated. For increasing the grain size of the final strips to obtain better creep properties as well as improved resistance to fatigue crack growth,²⁵ the alloy was solution annealed at a supersolvus temperature. Solution annealing temperature and time were 1145°C and 4 h respectively, after which the strips were cooled in air and exposed to two different aging cycles. A series of samples were first aged at 1000°C for 4 h and then aged at 850°C for 16 h and finally aged at 760°C for 16 h, all of them followed by air cooling. This heat treatment is coded as type A heat treatment in the present research. Another series of samples were aged at 850°C for 24 h and then aged at

760°C for 16 h. This heat treatment is coded as type B heat treatment.

Some of the cast ingots were heat treated after casting (without hot working) to compare the mechanical properties as well as the microstructure of the IN939 superalloy in the cast and wrought conditions. For the cast specimens, the solution temperature and time were 1150°C and 4 h respectively. A series of specimens were air cooled after solution treatment and aged according to the four-stage standard heat treatment schedule. This four-stage treatment includes one solution and three successive aging cycles.^{5–7} Aging of such materials was performed at 1000°C for 6 h followed by air cooling and subsequent aging at 900°C for 24 h and final aging at 700°C for 16 h. Another series of cast samples were furnace cooled after solution annealing at the rate of $\sim 20^\circ\text{C min}^{-1}$. These materials were finally aged at 850°C for 16 h and then air cooled.

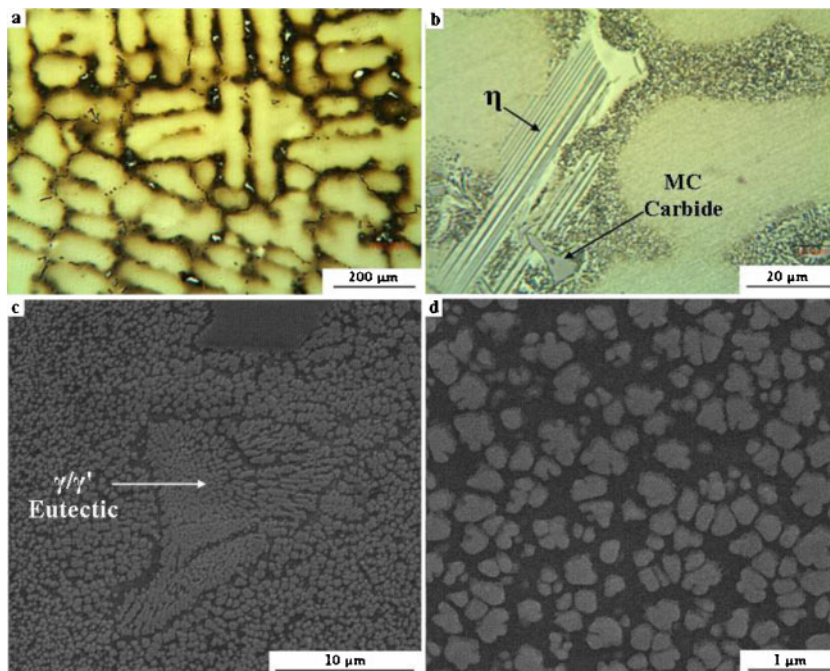
Tensile and stress rupture test specimens were machined from hot rolled strips as well as cast bars after heat treatment. For the hot rolled parts, these specimens were machined from the middle of the strips so that the rolling direction was parallel to the tension axis in all mechanical tests. Tensile tests were performed according to standards ASTM-E8 and ASTM-E21 in the range of 25–850°C, and stress rupture tests were conducted according to ASTM-E139 standard at temperatures and stresses in ranges of 750–900°C and 170–500 MPa correspondingly. Moreover, the microstructure of materials was analysed by optical and scanning electron microscopies after the preparation of metallographic samples.

Results and discussion

Figure 1 shows the alloy microstructure in the as cast condition. The alloy has a dendritic microstructure. The microstructure of the cast parts includes the matrix γ together with other precipitated phases such as γ' particles, MC carbides and some η phases. MC carbides, γ/γ' eutectics and platelets of η phase have been generally formed in the interdendritic regions of the microstructure. γ' particles have a variety of sizes and shapes in the dendrite cores or interdendritic regions. Some rose-like γ' precipitates can be seen in the interdendritic regions with sizes in the range of 0.5–1 μm .

Figure 2 shows the microstructure of the cast parts after heat treatments. Although the homogeneity of the cast alloy has been increased to some extent, there is still a considerable amount of inhomogeneity in the microstructure. The dendritic form of the microstructure has remained, and there is a large amount of η phase in the microstructure. γ' particles have larger size in the samples that were furnace cooled after solution annealing. Quantitative metallography showed that the volume fraction of γ' precipitates is around 32–36%.

Figure 3 shows the alloy microstructure after homogenisation annealing and final hot rolling. Figure 4 shows the final microstructure of the wrought alloy after heat treatments with two different aging cycles. These figures indicate that the grain size of the hot rolled specimens is much finer than those of the cast and homogenised samples. This indicates that the recrystallisation has occurred during hot rolling or reheating cycles. The IN939 superalloy has large amounts of Co and Cr. This can decrease the stacking fault energy of

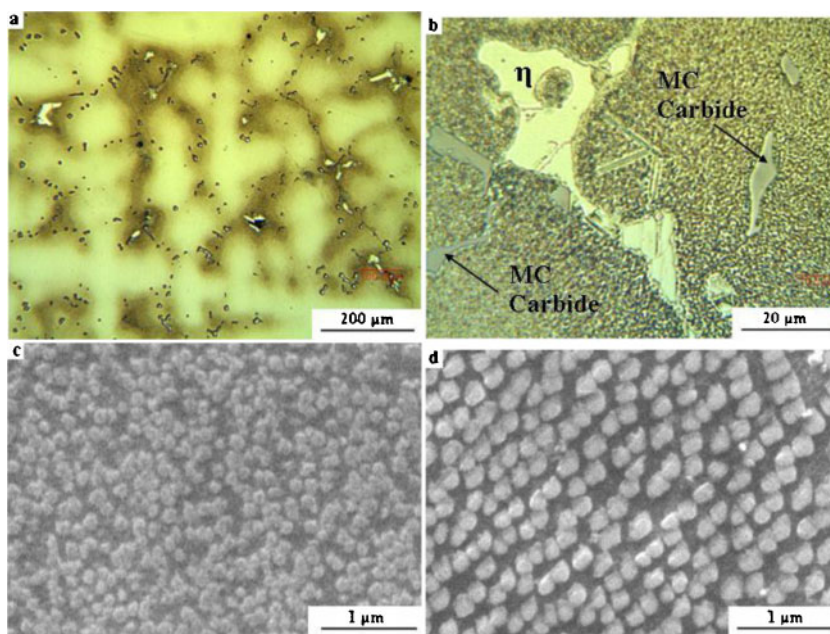


1 Microstructures of cast specimens: *a* dendritic appearance of microstructure and presence of *b* η phase and MC carbides, *c* γ/γ' eutectics and *d* rose-like γ' particles in interdendritic regions

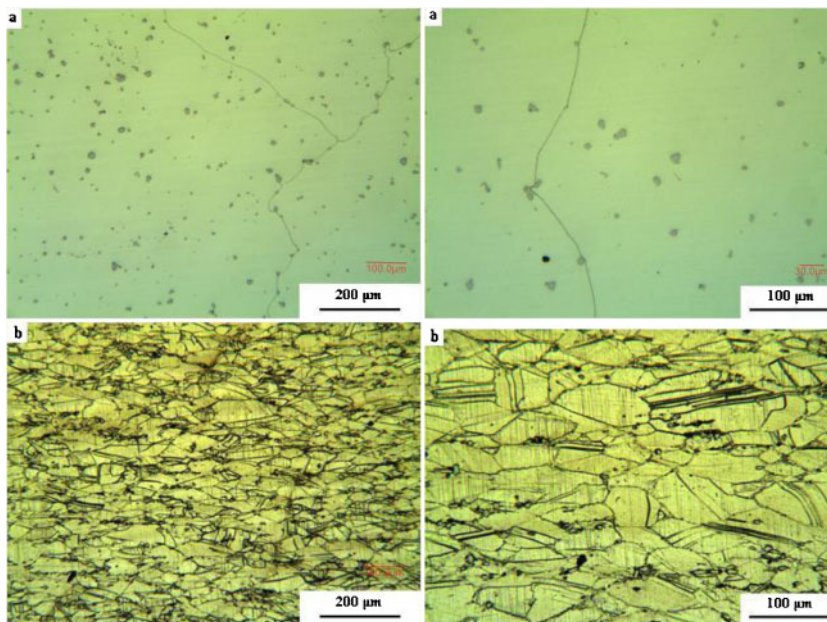
the alloy.²⁶ At elevated temperatures, alloys having low SFE can easily undergo dynamic recrystallisation during thermomechanical processing.

The final hot rolled samples have pancake and elongated grains in the rolling direction. This shows that recrystallisation has not been completed during final hot rolling at 1050°C or subsequent air cooling. As a result, during final hot rolling procedure at 1050°C, dynamic recovery and/or work hardening are the main microstructural change micromechanisms, and these can lead to an increase in dislocation density and hardness of the alloy along with the formation of subgrain boundaries.²⁷

After solution annealing at 1145°C and two different types of aging, the wrought alloy microstructure has been statically recrystallised, and the grain size was obtained in the range of 80–100 μm. No residual coarse primary γ' particle within the microstructures was observed. This is due to the use of high temperature homogenisation annealing cycle before hot rolling and utilising supersolvus solution cycle after hot rolling procedure. In addition, no residual η phase was observed in the microstructure of homogenised cast bars or final heat treated wrought alloys. This indicates that unlike the standard solution annealing used for cast



2 Microstructures of cast specimens after *a-c* four-stage standard heat treatment and *d* furnace cooling after solution annealing and aging at 850°C for 16 h



a cast and homogenised; b hot rolled

3 Microstructures of specimens

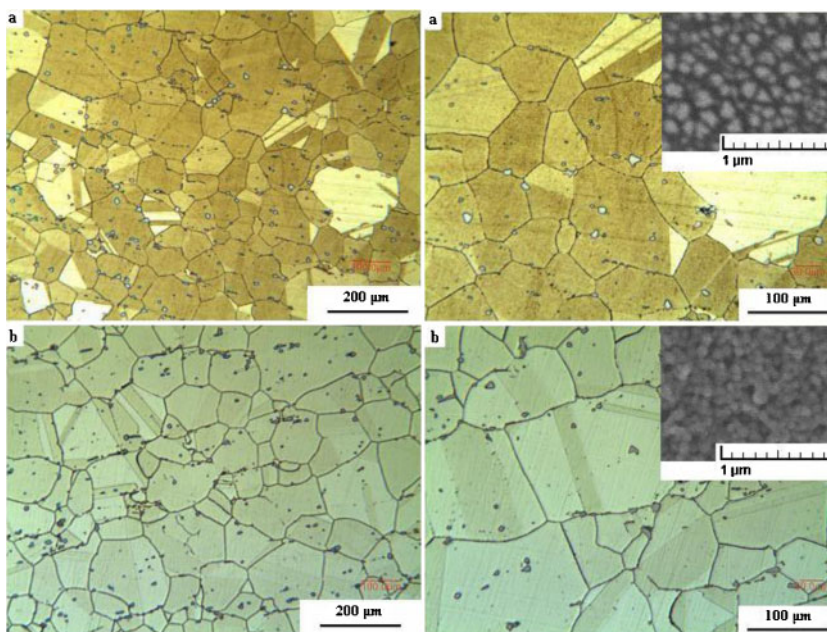
ingots, the selected two-stage homogenisation annealing was able to dissolve the η phase completely.

A significant point is the presence of numerous twins in the microstructures of wrought materials. These twins, which have been produced during hot rolling and heat treatments, indicate that twinning is a major deformation mechanism of this alloy at high temperatures. These twins can play a significant role in enhancing the alloy strength,^{28,29} while they can affect the dynamic recrystallisation of the alloy³⁰ as well as the precipitation of γ' and carbide particles.

Figure 5 shows the tensile properties of wrought and cast IN939 alloys after final heat treatments. Wrought samples heat treated according to type A heat treatment had a bimodal γ' size distribution (Fig. 6a) with average

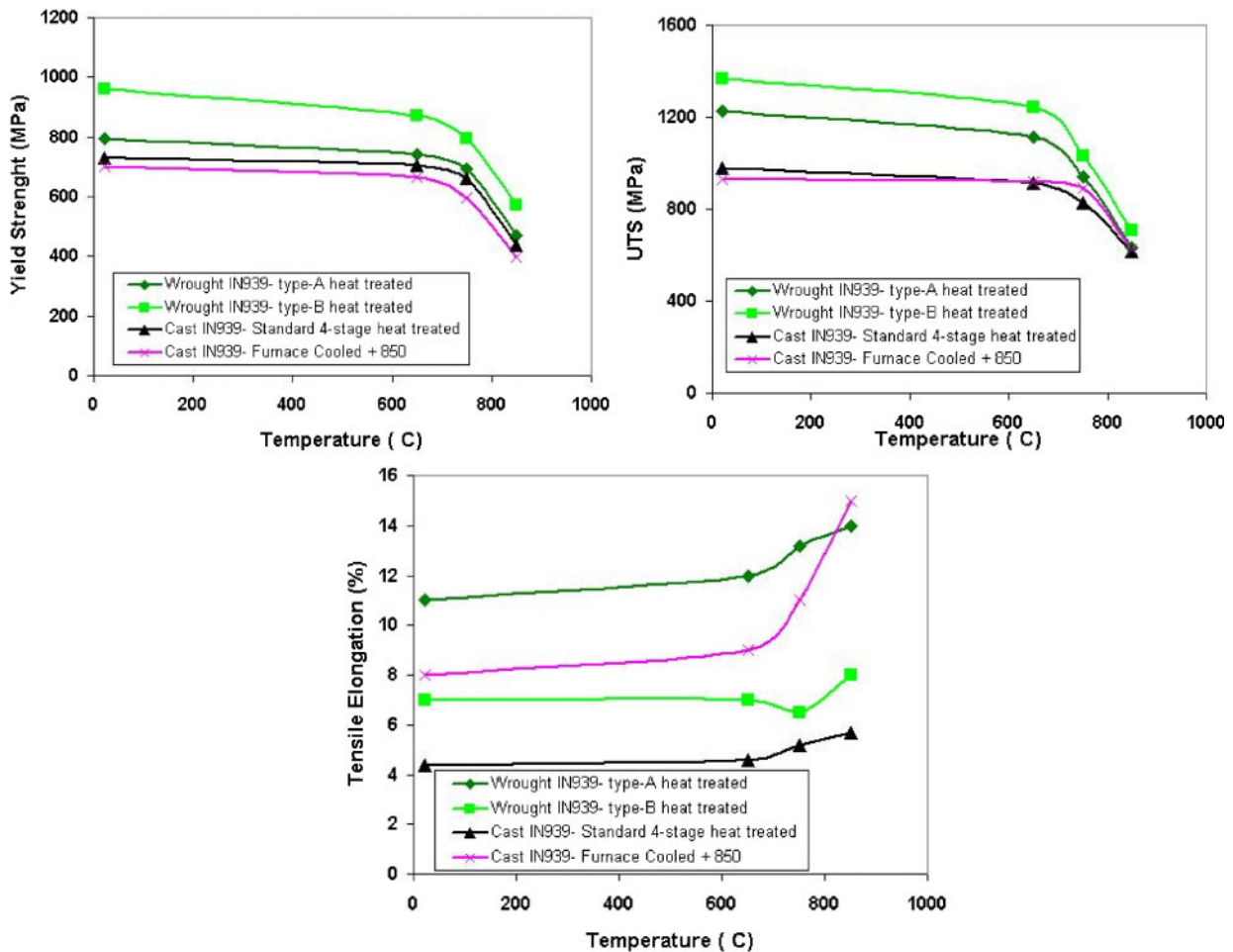
sizes of 50 and 130 nm respectively. Since γ' is the major strengthening phase in IN939 superalloy, the strengthening effects of these γ' particles can be significantly reduced by particle coarsening during first step aging at 1000°C. This explains why the type A heat treated samples with a bimodal distribution of γ' had lower yield and tensile strength than those heat treated according to the type B heat treatment having fine (in the range of 50–75 nm) γ' particles (Fig. 6b). The volume fraction of γ' precipitates was calculated to be ~35% for the wrought samples.

As shown in Fig. 5, the yield strength, ultimate tensile strength and ductility of wrought IN939 material are superior to the cast version. These conditions are almost true for all temperatures except for those cast samples,



a type A heat treated; b type B heat treated

4 Microstructures of wrought specimens

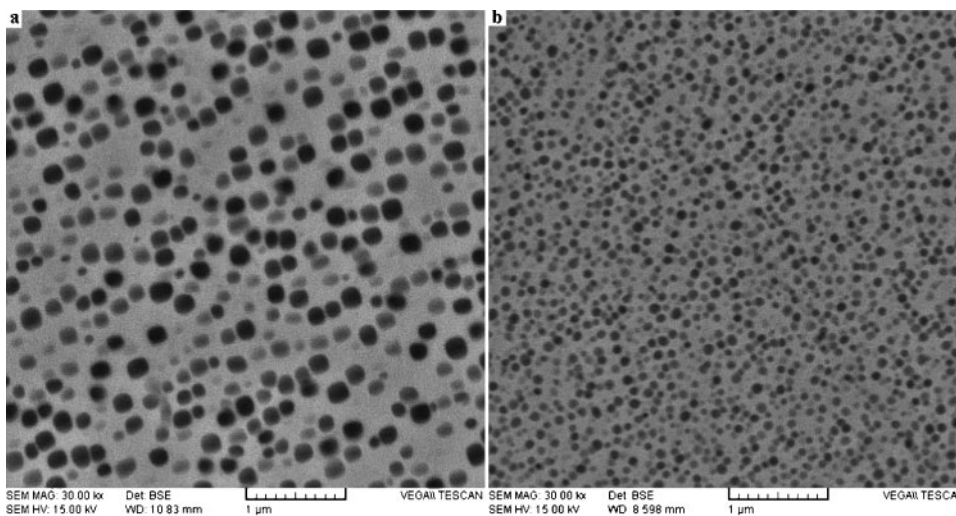


5 Comparison of tensile properties of IN939 superalloy in cast and wrought conditions

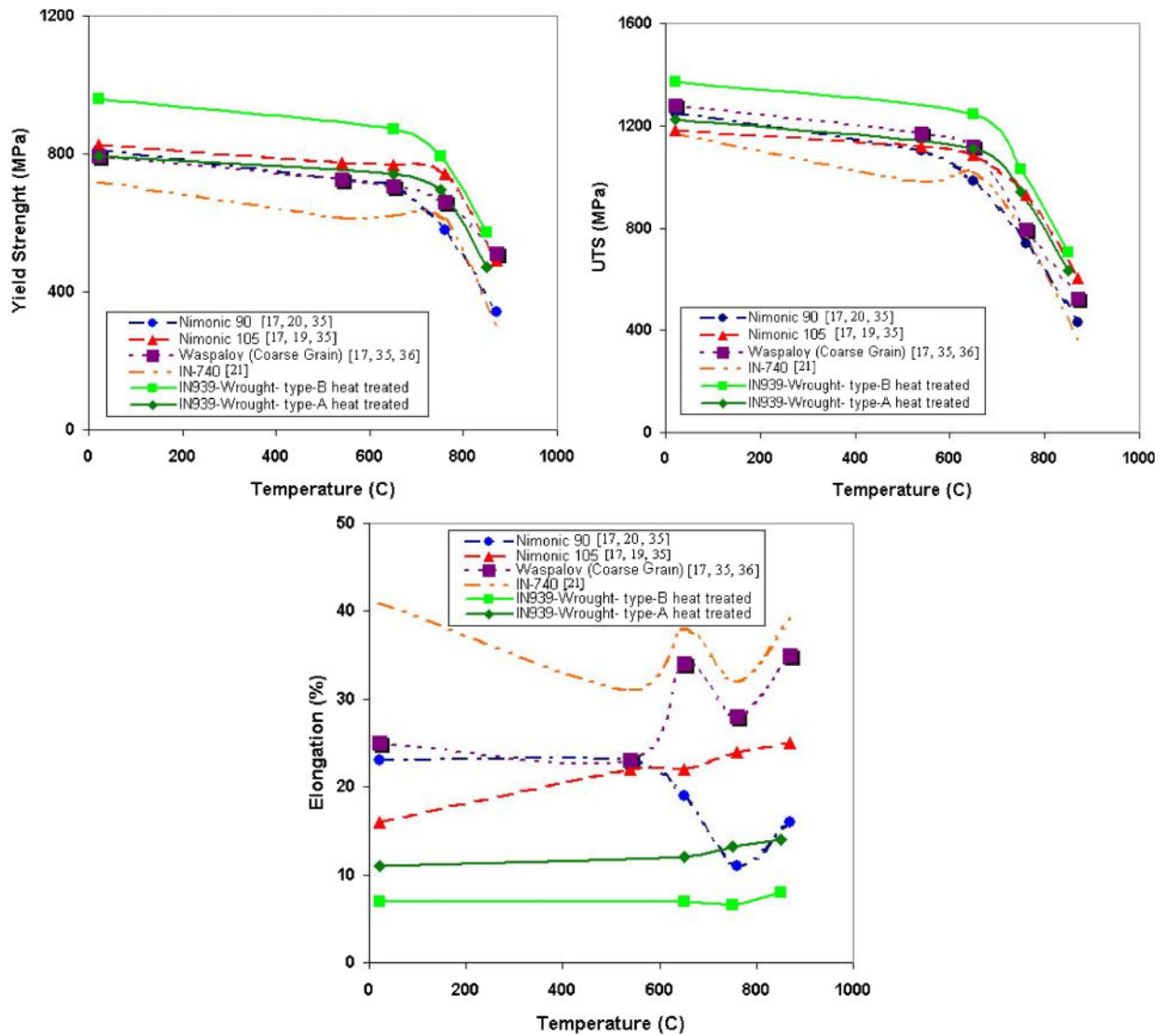
which were furnace cooled after solution annealing. These samples showed, to some extent, better ductility with respect to the wrought alloys heat treated according to the type B heat treatment.

Since the overall chemical composition of the alloy is the same for both cast and wrought samples, the superior tensile properties of the wrought IN939 alloy can be attributed to its more homogeneity and finer microstructure relative to the cast sample. Grain

boundaries act as dislocation barriers, and decreasing the grain size can increase the tensile strength of the wrought alloy. On the other hand, a reduction in grain size can improve ductility by activation of multiple slip systems. As multiple slip is almost common in the vicinity of grain boundaries,^{31,32} the smaller the grain size, the more uniform the deformation, and this leads to better ductility during deformation. These observations have been also reported for other superalloys.^{10,15,33}



6 Microstructures of γ' precipitates in a type A heat treated wrought IN939 alloy and b type B heat treated wrought IN939 alloy



7 Comparison of tensile properties of wrought IN939 alloy with other selected wrought precipitation strengthened superalloys

Moreover, complete dissolution of the η phase during two-stage homogenisation annealing has resulted in better tensile properties. It has been shown that η phase has a detrimental effect on the mechanical properties of IN939 superalloy, especially its ductility.^{4,34}

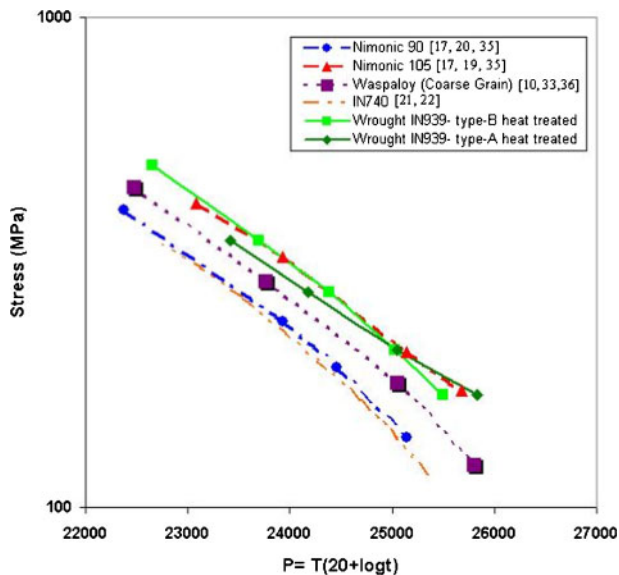
Comparison of the tensile properties of wrought IN939 alloy obtained in the present research with those of the other conventional wrought superalloys reported in various references^{10,12,17,19–22,33,35,36} is illustrated in Fig. 7. This figure shows that the yield and ultimate tensile strengths of type B heat treated wrought IN939 alloy are more than that of the selected widely used superalloys at all temperatures. The yield strength of type A heat treated wrought IN939 alloy is somewhat less than that of Nimonic 105 up to 750°C, but this

property approaches Nimonic 105 and Waspaloy at higher temperatures.

The higher yield strength of the type B heat treated wrought IN939 superalloy compared to Waspaloy, Nimonic 90 and IN740 superalloys seems to have resulted from its chemical composition, as it contains more Ti, Al, Nb and Ta relative to the other mentioned alloys. These alloying elements produce more γ' particles and improve the yield strength of the alloy.^{15,16,37} Table 1 compares the chemical composition and volume fractions of γ' particles for the selected superalloys. The superior yield strength of the type B heat treated wrought IN939 superalloy compared to the Nimonic 105 superalloy can be attributed to its more Ti and Co contents and higher Ti/Al ratio according to Xu *et al.*,¹¹

Table 1 Typical chemical composition and volume fractions of γ' particles for different superalloys (wt-%)

Alloy	Ni	C	Co	Cr	Ti	Al	W	Ta	Nb	Zr	B	γ' /vol.-% (reference)
IN939	Balance	0.14	19.5	22.5	3.7	1.9	2	1.5	1	0.1	0.01	35 (the present work)
Ni-105	Balance	0.14	20	15	1.3	4.7	–(Mo:5)	0.1	0.01	45 (Refs. 42 and 43)
Ni-90	Balance	0.1	17.5	19.5	2.5	1.5	0.1	0.01	19.6 (Ref. 53)
Waspaloy	Balance	0.06	13.5	20	3	1.4	–(Mo:4)	0.1	0.008	25–30 (Ref. 54)
IN740	Balance	0.03	20	25	1.8	0.9	–(Mo:0.5)	...	2	20–25 (Ref. 55)



8 Comparison of stress rupture properties of wrought IN939 alloy with other selected wrought precipitation strengthened superalloys

Sims *et al.*¹² and Cui *et al.*³⁷ and probably finer γ' particles in the former alloy.³⁸ As mentioned earlier, increasing the temperature of the first step of aging cycle lowered the yield strength of the type A heat treated wrought IN939 alloy due to the coarsening effect that the duration of this step had on γ' precipitates.

The ultimate tensile strength of Waspaloy is somewhat superior to the type A heat treated wrought IN939 alloy up to 650°C. This is because of the finer γ' particles presented in the Waspaloy microstructure. Because Waspaloy is aged at 850 and 760°C respectively, these temperatures would result in finer γ' particles compared to higher aging temperatures used for type A heat treated wrought IN939 alloy. These fine particles can enhance the tensile strength of superalloys at low and moderate temperatures.^{12,15,33,39} At higher temperatures, the ultimate tensile strength of the type A heat treated alloy is nearly the same as that of Nimonic 105 alloy but more than those of the other selected wrought superalloys such as Waspaloy, Nimonic 90 and IN740.

Comparison of alloy ductilities at various temperatures illustrated in Fig. 7 shows that this property is steadier for the two types of heat treated wrought IN939 superalloys at all temperatures with respect to the other alloys. Although the type A heat treated material has better ductility than type B, both types have desirable ductilities (i.e. $\geq 6\%$) at all temperatures.

Figure 8 compares the stress rupture properties of the two-type heat treated wrought IN939 superalloys with the other selected conventional superalloys.

It is well known that during creep of superalloys, three essential interactions occur between dislocations and γ' particles: shearing of γ' by dislocations, looping of dislocations around γ' particles and dislocation climb around γ' .^{1,10,15} At low temperatures and high stresses, shearing and looping mechanisms are prevalent, while at high temperatures and low stresses, looping and climb are dominant.^{40,41}

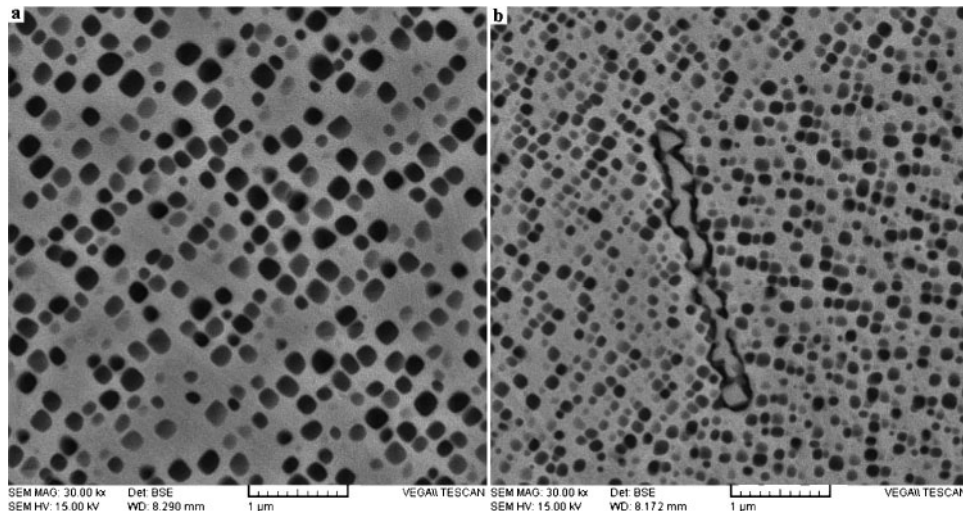
Type B heat treatment for wrought IN939 alloy yields appropriate high stress and short time rupture properties

but did not stabilise the microstructure sufficiently to produce optimised rupture properties for long time high temperature services. Owing to the instability of fine γ' particles that existed in type B wrought alloy at high temperatures, dislocations can easily climb around these particles. The use of a higher temperature in the first step of aging cycle (i.e. 1000°C for 4 h) for the type A heat treated alloy can lead to the stabilisation of microstructure and better long term, low stress, high temperature rupture properties. The positive effect of an intermediate aging cycle on the long time creep properties of other wrought superalloys has been documented previously in Refs. 10, 12 and 17.

As shown in Fig. 8, the stress rupture properties of wrought IN939 superalloy are better than those of most of the selected superalloys (Waspaloy, Nimonic 90 and IN740) and approach the alloy Nimonic 105 properties. Since the IN939 superalloy contains higher γ' volume fraction compared to Waspaloy, Nimonic 90 and IN740 superalloys (Table 1), the superiority of its creep resistance was predictable. However, the equality of creep properties of Nimonic 105 and wrought IN939 is very notable because Nimonic 105 contains ~ 45 vol.-% γ' ^{42,43} that is much greater than the volume fraction of those precipitates in the alloy IN939 ($\sim 35\%$).

The creep resistance of precipitation strengthened superalloys is controlled by various parameters, including volume fraction, chemical composition and size of γ' precipitates along with the grain size of the alloy.^{10,12,15,17,33} Because Nimonic 105 and wrought IN939 superalloys have been solution annealed at supersolvus conditions, the grain size of two alloys is identical in the range of 80–100 μm .^{35,42,43} Comparison of the chemical composition of the two alloys shows that IN939 alloy has more strengthening elements, such as Ti, Ta, Nb, W and Cr in its composition except the elements Al and Mo, which are less than those existing in Nimonic 105 alloy. Both of these alloys have the same contents of Co, C, B and Zr. The results show that although the existence of more Al content in the Nimonic 105 alloy composition can lead to the formation of more γ' particles (i.e. higher volume fraction of γ'), the potential of the Al enriched particles to enhance the creep properties of the alloy is less than that of the particles having elements such as Ti, Nb, Ta and W, as reported by other researchers.^{10,11,44–46} Moreover, it has been reported that the coarsening (ripening) rate of γ' particles during creep of superalloys decreases as the Cr and Co contents of the alloy increased.^{11,12,47} Consequently, these elements, which have high concentration in IN939 superalloy, reduce the solubility of Al and Ti in γ phase and hence decrease the γ' particles' growth rate. This stabilises the microstructure of IN939 alloy compared to Nimonic 105. It has been also shown that the presence of Ta, W and Nb elements in superalloys can decrease the coarsening rate of γ' particles due to their low diffusivity in the γ matrix.^{44,48,49} Because IN939 superalloy has high amounts of these slow diffusing elements, the coarsening rate of γ' particles in the IN939 superalloy is lower than that in the Nimonic 105 alloy. This can also enhance the creep resistance of wrought IN939 superalloy at high temperatures and long times.

Figure 9 shows the microstructure of type A and B heat treated wrought IN939 superalloys after 1500 h



9 Microstructures of γ' precipitates after 1500 h aging at 800°C for a type A wrought IN939 alloy and b type B wrought IN939 alloy

aging at 800°C. It can be seen that the type A heat treated alloy has a more stable microstructure, as the coarser γ' particles formed during the first stage of aging cycle are almost unchanging even after long times. Some twin planes decorated with $M_{23}C_6$ carbides are also observed in Fig. 9b.

Finally, it can be considered that the higher volume fraction of MC carbides in the IN939 alloy microstructure (see Figs. 3 and 4) due to the presence of more MC carbide forming elements such as Ti, Ta and Nb relative to the Nimonic 105 alloy can lead to the improvement of creep properties. The beneficial effect of these MC carbides on the creep and tensile properties of superalloys has been established in other works.^{50–52}

Conclusions

In the present work, the wrought version of the cast IN939 superalloy was developed. Through microstructural and mechanical property experiments on cast and wrought IN939 superalloys with two different types of heat treatments, the following conclusions can be drawn.

1. The yield strength, ultimate tensile strength and ductility of the wrought IN939 superalloy are better than that of the cast version.

2. The stress rupture properties of wrought IN939 superalloy are superior to those of the widely used superalloys such as Nimonic 90 and Waspaloy and approach the alloy Nimonic 105 properties. This is very important because the γ' volume fraction of the IN939 alloy is much less than the γ' volume fraction of the Nimonic 105 alloy.

3. The wrought IN939 superalloy has a stable microstructure at high temperatures. Type A heat treated alloy is more stable because of using a higher temperature for the first stage of the aging cycle.

4. Considering the excellent corrosion resistance of the IN939 alloy together with the good weldability and mechanical properties, the wrought version of this alloy would have a high potential to be used at high temperatures.

References

1. M. J. Donachie: 'Selection of metals for structural design', in 'Eshbach's handbook of engineering fundamentals', (ed M. Kutz), Chap. 4, 5th edn; 2009, Hoboken, NJ, John Wiley & Sons, Inc, 358–391.

2. C. Rae: *Mater. Sci. Technol.*, 2009, **25**, (4), 479–487.
3. R. F. Decker: *JOM*, 2006, **58**, (9), 32–36.
4. K. Harris and J. B. Wahl: *Mater. Sci. Technol.*, 2009, **25**, (2), 147–153.
5. T. B. Gibbons and R. Stickler: in 'High temperature alloys for gas turbines', (ed R. Brunetaud *et al.*), 369–393; 1982, Dordrecht, D. Reidel Publishing.
6. S. W. K. Shaw: 'Superalloys 1980', 275–284; 1980, Materials Park, OH, ASM.
7. K. M. Delargy, S. W. K. Shaw and G. D. W. Smith: *Mater. Sci. Technol.*, 1986, **2**, 1031–1037.
8. C. Y. Cui, Y. F. Gu, D. H. Ping, H. Harada and T. Fukuda: *Mater. Sci. Eng. A*, 2008, **A485**, 651–656.
9. Y. Murata, R. Hashizume, A. Yoshinari, N. Aoki, M. Morinaga and Y. Fukui: 'Superalloys 2000', 285–294; 2000, Warrendale, PA, TMS.
10. J. R. Davis: 'ASM specialty handbook: Heat resistant materials'; 1997, Materials Park, OH, ASM International.
11. L. Xu, C. Cui and X. Sun: *Mater. Sci. Eng. A*, 2011, **A528**, (27), 7851–7856.
12. C. T. Sims, N. S. Stoloff and W. C. Hagel: 'Superalloys II'; 1987, New York, John Wiley & Sons.
13. V. Biss, G. N. Kirby and D. L. Sponseller: *Metall. Trans. A*, 1976, **7A**, (9), 1251–1261.
14. D. R. Malley: US Patent 5,938,863, 1999.
15. R. C. Reed: 'The superalloys: fundamentals and applications'; 2006, Cambridge, Cambridge University Press.
16. J. P. Collier, P. W. Keefe and J. K. Tien: *Metall. Trans. A*, 1986, **17A**, 651–661.
17. E. F. Bradley: 'Superalloys: a technical guide'; 1988, Materials Park, OH, ASM International.
18. O. A. Ojo: *Mater. Sci. Technol.*, 2007, **23**, (10), 1149–1155.
19. 'Nimonic alloy 105 product specifications', Publication no. SMC-081, Special Metals Corporation, New Hartford, NY, USA, 2007.
20. 'Nimonic alloy 90 product specifications', Publication no. SMC-080, Special Metals Corporation, New Hartford, NY, USA, 2004.
21. Inconel alloy 740 product specifications, Publication no. SMC-090, Special Metals Corporation, New Hartford, NY, USA, 2004.
22. S. Sridhar, P. Rozzelle, B. Morreale and D. Alman: *Metall. Mater. Trans. A*, 2011, **42A**, 871–877.
23. Z. J. Miao, A. D. Shan, J. Lu and H. W. Song: *Mater. Sci. Technol.*, 2011, **27**, (10), 1551–1557.
24. P. D. Jablonski and C. J. Cowen: *Metall. Mater. Trans. B*, 2009, **40B**, 182–186.
25. T. P. Gabb, P. T. Kantzos, J. Telesman, J. Gayda, C. K. Sudbrack and B. Palsa: *Int. J. Fatigue*, 2011, **33**, (3), 414–426.
26. Y. Yuan, Y. Guo, C. Cui, T. Osada, Z. Zhong, T. Tetsui, T. Yokokawa and H. Harada: *J. Mater. Res.*, 2011, **26**, 2833–2837.
27. N. D. Ryan and H. J. McQueen: *Mater. Sci. Eng.*, 1986, **81**, 259–272.
28. Y. Yuan, Y. Gu, C. Cui, T. Osada, T. Yokokawa and H. Harada: *Adv. Eng. Mater.*, 2011, **13**, (4), 296–300.
29. L. L. Shaw, J. Villegas, J. Y. Huang and S. Chen: *Mater. Sci. Eng. A*, 2008, **A480**, (1–2), 75–83.

30. D. Li, Q. Guo, Sh. Guo, H. Peng and Zh. Wu: *Mater. Des.*, 2011, **32**, (2), 696–705.
31. R. J. Asaro and V. A. Lubarda: 'Mechanics of solids and materials'; 2006, Cambridge, Cambridge University Press.
32. G. E. Dieter, H. A. Kuhn and S. L. Semiatin: 'Handbook of workability and process design'; 2003, Materials Park, OH, ASM International.
33. M. J. Donachie and S. J. Donachie: 'Superalloys: a technical guide', 2nd edn; 2002, Materials Park, OH, ASM International.
34. J. B. Wahl and K. Harris: *Can. Metall. Q.*, 2011, **50**, (3), 207–214.
35. W. Betteridge: 'The nimonic alloys and other nickel-base high-temperature alloys'; 1974, London, Edward Arnold Limited.
36. 'Waspaloy product specifications', Publication no. SMC-011, Special Metals Corporation, New Hartford, NY, USA, 2004.
37. C. Y. Cui, Y. F. Gu, H. Harada, D. H. Ping and A. Sato: *Metall. Mater. Trans. A*, 2006, **37A**, 3183–3190.
38. H. J. Sharpe and A. Saxena: *Adv. Mater. Res.*, 2011, **278**, 259–264.
39. S. Sinharoy, P. Virro-nic and W. W. Milligan: *Metall. Mater. Trans. A*, 2001, **32A**, 2021–2032.
40. R. R. Unocic, G. B. Viswanathan, P. M. Sarosi, S. Karthikeyan, J. Li and M. J. Mills: *Mater. Sci. Eng. A*, 2008, **A483–A484**, 25–32.
41. M. Huang, L. Zhao and J. Tong: *Int. J. Plast.*, 2012, **28**, (1), 141–158.
42. B. Reppich, P. Scheppard and G. Wehner: *Acta Metall.*, 1982, **30**, (1), 95–104.
43. A. Nitz and E. Nembach: *Mater. Sci. Eng. A*, 1997, **A234–A236**, 684–686.
44. M. Sundararaman: *Miner. Process. Extr. Metall. Rev.*, 2002, **22**, (4–6), 681–700.
45. A. K. Jena and M. C. Chaturvedi: *J. Mater. Sci.*, 1984, **19**, 3121–3139.
46. Y. F. Gu, C. Cui, D. Ping, H. Harada, T. Fukuda and J. Fujioka: *Mater. Sci. Eng. A*, 2009, **A510–A511**, 250–255.
47. G. P. Salel and R. Stickler: *Phys. Status Solidi*, 1969, **35**, (4), 11–52.
48. M. Durand-Charre: 'The microstructure of superalloys'; 1997, Amsterdam, Gordon and Breach Science Publishers.
49. M. Gebura and J. Lapin: *Defect Diffus. Forum*, 2010, **297–301**, 826–831.
50. F. S. Yin, X. F. Sun, J. G. Li, H. R. Guan and Z. Q. Hu: *Mater. Lett.*, 2003, **57**, (22–23), 3377–3380.
51. K. Zhao, Y. H. Ma and L. H. Lou: *J Alloys Compd*, 2009, **475**, (1–2), 648–651.
52. C. N. Wei, H. Y. Bor and L. Chang: *Mater. Sci. Eng. A*, 2010, **A527**, (16–17), 3741–3747.
53. X. Li, N. Saunders and A. P. Miodownik: *Metall. Mater. Trans. A*, 2002, **33A**, 3367–3373.
54. L. Naze and J. L. Strudel: *Mater. Sci. Forum*, 2010, **638–642**, 53–60.
55. C. J. Cowen, P. E. Danielson and P. D. Jablonski: *J. Mater. Eng. Perform.*, 2011, **20**, (6), 1078–1083.